STUDY ON PERFORMANCE OF GEOCELL REINFORCED FOUNDATION BEDS WITH DIFFERENT TYPE OF GEOCELLS

Sujit Kumar Dash[1]

[1] *Indian Institute of Technology Guwahati, Guwahati -781 039. (e-mail: sujit@iitg.ernet.in)*

Abstract: Under the present research work a detailed experimental investigation has been carried out to study the influence of stiffness, aperture opening size and orientation of ribs of the geogrid material used to form the geocells, on the overall performance of geocell reinforced sand beds under strip loading. Three types of geogrids with different stiffness and aperture openings were used for making the geocells. One was a biaxial grid (BX) made of oriented polymer while the other two were made of non-oriented polymers (NP-1 and NP-2).

The test results indicate that the tensile strength of the geogrid used to make geocells, alone, is not a sufficient parameter. The aperture opening size and the orientation of the ribs too should be taken into account while evaluating the performance of a geocell foundation mattress.

Keywords: bearing capacity, earth reinforcement, geocell.

INTRODUCTION

Reinforced-soil is one of the first growing techniques being used for treatment of foundation soil to improve its performance. The more recent advancement in this field is to provide three-dimensional confinement to the soil by using geocells. The beneficial effect of incorporating geocell in soil fills has been reported by several authors e.g. Bush et al. (1990), Cowland and Wong (1993), Krishnaswamy et al. (2000), Dash et al (2001).

Under the present research work a detailed experimental investigation has been carried out to develop an understanding of the influence of the stiffness, aperture opening size and orientation of ribs of the geogrid material used to form the geocells, on the overall performance of geocell reinforced sand beds under strip loading.

EXPERIMENTAL PROGRAMME

The model tests were conducted in a steel tank measuring 1200 mm length × 332 mm width × 700 mm height. The length sides of the tank were made of thick perspex sheet and were braced with angle iron to avoid yielding during the tests. The perspex wall apart from minimising the friction between the soil and the tank permitted observation of pattern of deformations of the sand during test. The model foundation used was made of steel and measured 330 mm length × 100 mm width × 25 mm thickness. A rough-base condition was achieved by cementing a thin layer of sand onto the base of the model foundation with epoxy glue. The footing was centered in the tank, with the length of the footing parallel to the width of the tank. Since the length of the footing is almost equal to the width of the test tank a plane strain condition was generally maintained during the tests. On each side of the tank a 1 mm gap was given to prevent contact between the footing and the sidewalls.

The soil used is a uniformly graded river sand (SP) with properties C_u = 2.318, C_c = 1.03, D_{50} = 0.46mm, γ_{max} = 17.41 kN/m^3, γ_{min} = 14.30 kN/m^3. Tests were carried out at relative density (ID) of 70%. The peak friction angle of the sand at relative density of 70% as determined from direct shear tests is 46°. Three different types of geogrids were used for forming the geocells. One was a biaxial grid (BX) made of oriented polymer while the other two were made of non-oriented polymers, referred to as NP-1 and NP-2 grid. These geogrids were chosen in order to have varying tensile strength, aperture opening size and shape. The properties of the geogrids were determined from the standard wide width tension tests carried out as per ASTM D4595. These properties and aperture size of the geogrids are listed in Table 1.

Table 1. Properties of the geogrids

Property	Value		
	BX	**NP-1**	**NP-2**
Ultimate tensile strength (kN/m)	20	4.5	7.5
Failure strain (%)	25	10	55
Initial modulus (kN/m)	183	75	95
Secant modulus at 5% strain(kN/m)	160	70	70
Secant modulus at 10% strain(kN/m)	125	45	50
Aperture size (mm)	35×35	50×50	8×7
Shape of aperture opening	square	square	diamond

The geocell mattresses were prepared by placing the geogrid strips in transverse and diagonal directions with bodkin joints (i.e. plastic strips) inserted at the connections (Bush et al.1990). To achieve uniform density in the fill soil, sand-raining technique was used. By varying the free fall of dispersed sand particles, the placement density of the sand was varied. The accuracy of sand placement and consistency of the placement density were checked during raining by placing small aluminum cans with known volumes at different locations in the test tank. The difference in densities measured at various locations in the test tank was found to be less than 1%.

At desired depth as per test configuration, the sand raining was temporarily ceased and the reinforcement (i.e. geocell and/or planar) was placed on the surface of the sand. After this, sand raining was continued. It should be mentioned here that the reduction in placement density due to the presence of the geocell mattress was found to be less than 1%, which is negligible.

The footing was loaded by a hand operated hydraulic jack supported against a reaction frame. The load was applied incrementally. The load applied to the footing was measured through a pre-calibrated proving ring suspended from the spindle of the jack through an adapter and resting on the footing through a ball bearing. Settlements of the footing were measured by two dial gauges placed in diagonal directions. The deformations of the fill surface (heave/ settlement) on either side of the footing were measured by dial gauges. In many cases the number of load increments was more than 20. Each load increment was maintained constant until the footing settlement under that particular load increment has stabilised. In the absence of a clear-cut failure, the footing was driven to a maximum displacement of 50mm. The geometry of the problem is shown in Figure 1. The pocket size (d) of geocells is taken as the diameter of an equivalent circular area of geocell pocket opening. In all the tests the pocket size of the geocells (d), height of the geocell layer (h), width of the geocell layer (b) and depth of placement of geocell layer (u) were kept constant i.e. d/B = 1.6, h/B = 1.2, b/B = 8 and u/B = 0.1 respectively.

The strains developed in the geocell reinforcement were measured through electrical resistance-type-strain gauges of 10 mm gauge length fixed at various locations on the geocell walls. The vertical earth pressures below the geocell layer were measured using electrical resistance strain gauge type earth pressure cells. The deformation pattern of subgrade below the geocell layer was observed by placing thin horizontal layers of white coloured sand at 50 mm vertical intervals. On completion of each test, the deformed shape of the coloured lines at different depths, which indicates the pattern of deformation of the subgrade soil, was recorded by tracing on a transparent paper. For each test, the test bed was prepared afresh with new reinforcement.

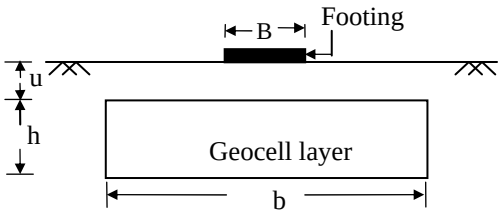

Figure 1. Geometric parameters of geocell reinforced foundation bed

RESULTS AND DISCUSSION

The influences of the type of geogrid (used to fabricate geocell mattress) on the footing performance are shown in Figures 2 and 3. Figure 2 depicts the pressure-settlement responses of the footing and Figure 3 depicts the deformations on the fill surface (settlement/heave) at different footing settlements.

The footing has shown almost equal bearing pressure with geocells made of BX and NP-2 grids up to a settlement equal to about 20% of the footing width. This is in spite of the stiffness of the BX grid being higher than that of the NP-2 grid (i.e. almost 2 times; Table 1). Since the aperture opening size of the NP-2 grid is almost 5 times smaller than that of BX grid (Table.1) it offers higher confinement to the encapsulated soil. Consequently, a better composite material is formed that redistributes the footing load over a wider area, giving rise to increased performance improvement. This could further be substantiated from the observation that, though both NP-1 and NP-2 grids have almost same stiffness, in the relatively lower settlement range (i.e. s/B ≤ 20%) the performance with NP-1 grids is comparatively inferior because of its higher aperture opening size.

From Figure 3 it could be observed that settlement of the fill surface is maximum in case of NP-2 geogrid. This finding indicates that the geocell earth bed made of NP-2 grid acts as a better composite body which enables it to deflect as a coherent mass under footing loading that establishes the higher confining efficiency of the geocells made of geogrid having smaller aperture openings.

Besides, the geocell mattress being an interconnected cage derives anchorage from both sides of the loaded area through mobilisation of interfacial friction between soil and reinforcement, interlocking of the soil through apertures of the geogrid and passive resistance through bearing at soil to grid cross bar interface. With decrease in aperture opening size of the geocell walls the effective reinforcement area available for mobilisation of anchorage from soil increases thereby giving rise to increased performance improvement.

At higher settlements, the performance with geocells made of BX grids is much better because of its higher stiffness. At this stage, sand starts moving out of the geocell pockets (as seen from Figure 3 in terms of surface heaving) and a larger portion of footing load gets directly transferred to the geocell wall, hence the stiffness of the geogrid influences the overall behaviour of the geocell mattress.

From Figure 2 it could be observed that in case of BX grid, the slope of the pressure settlement response is found to reduce at around 30% settlement of the footing. However, beyond that the bearing capacity once again continued to increase with increase in footing settlement. In case of NP-1 grid the pressure-settlement response undergoes a gradual change in slope and tends to become vertical beyond a settlement around 32% of the footing width. At higher settlement

the soil within the geocell pockets in the region below the footing overcomes interfacial friction and interlocking over the geocell wall and gets pushed down. With the shearing of encapsulated soil the geocell-soil composite structure breaks and hence substantial part of the footing load is directly transferred to the geocell matrix. At this stage the strength of the geocell material plays a dominant role in supporting the footing against the applied loads, through mobilisation of anchorage from both sides of the loaded area due to frictional, interlocking and soil passive resistance.

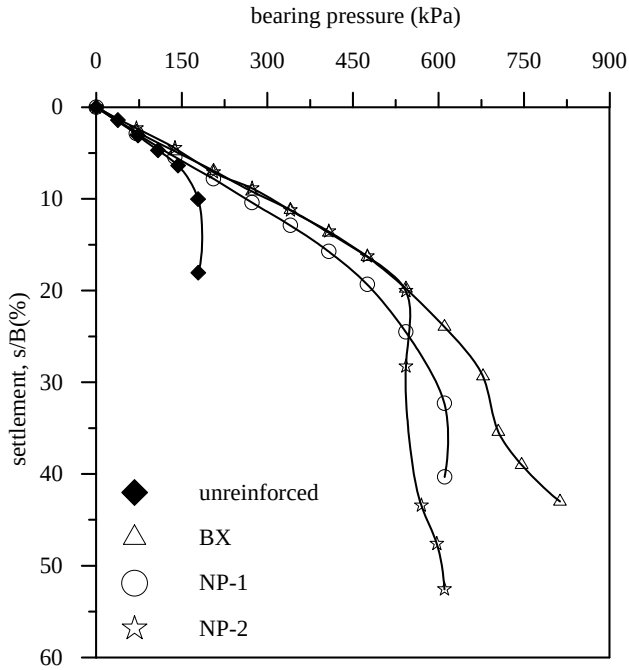

Figure 2. Bearing pressure-settlement responses of footing for different geocell materials

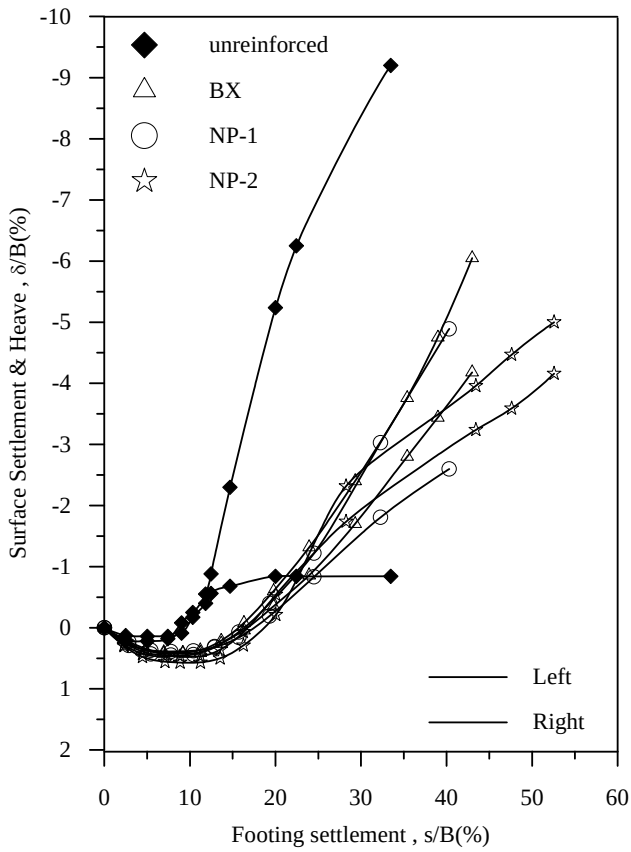

Figure 3. Deformation on fill surface-footing settlement responses for different geocell materials

The NP-1 grid having very low strength is found to have undergone severe yielding at joints, observed in the posttest exhumed geocell walls. With the shearing of soil and yielding of geocell walls the geocell soil matrix undergoes complete failure as observed in the pressure-settlement response. Whereas, the BX-grid being of very high strength the

geocell matrix continues to support the footing even after shearing of the encapsulated soil. The visible reduction in slope of the pressure-settlement response at around 30% settlement is due to the shearing of the encapsulated soil. Once the encapsulated soil shears the footing rests on the geocell matrix that enables to further carry load as observed in the pressure settlement response.

In case of geocells made of NP-2 geogrid, a sudden change in slope in the pressure-settlement response is observed at a settlement around 20% of the footing width. Beyond this settlement the pressure settlement curve is almost vertical indicating that the foundation bed has undergone a sudden failure. This is because in case of BX and NP-1 grid the aperture opening shape being square the ribs are in horizontal and vertical direction in the geocell wall that they effectively resist against footing penetration through mobilisation of vertical compression and horizontal anchorage. Whereas the ribs of NP-2 geogrid are in inclined direction (owing to diamond shape of its aperture opening) are unable to resist effectively the vertical compression from footing in post soil shearing stage. Indeed in the posttest observation, upon removal of top cushion of sand, the geocell walls (of NP-2 geogrids) were found to have folded under the footing. Whereas, in the other two cases (i.e. BX and NP-1) the geocell walls had been heavily deformed and buckled. This folding of the geocell walls is believed to have caused the early failure of the footing in the case of NP-2 geogrids.

Table 2. Strain, ε_h(%) measured at center of geocell mattress

BPR	Type of geogrid used to fabricate geocell		
	NP1	**BX**	**NP2**
0.378	0.081	0.028	-0.083
0.757	0.228	0.090	-0.127
1.136	0.380	0.172	-0.140
1.515	0.592	0.286	-0.175
1.894	0.850	0.410	-0.185
2.273	1.172	0.587	-0.214
2.652	1.661	0.863	-0.221

The values of strains measured at center of the geocell layer at different footing load levels (BPR) are presented in Table 2, wherein, (+) sign indicates tension and (-) sign indicates compression. The bearing pressure ratio (BPR) is defined as the ratio between the footing pressures with reinforced soil to the ultimate footing pressure in the unreinforced soil. It could be observed from Table 2 that the strains in NP1 grid are much higher than in BX grid. This can be directly related to the lower stiffness of NP1 geogrid than that of BX geogrid. The compression in NP2 grid indicates that its tensile strength remains not mobilised.

It was observed that in pre-failure stage the pressure transmitted to the base of the geocell mattress increases with decrease in aperture opening of the geogrid (i.e. NP1 > BX > NP2, see Table 1). This may be directly related to the higher confinement offered to the soil due to the smaller aperture openings of the geogrid used to fabricate the geocell. Such a confinement induces higher compressive strength to the encapsulated soil thereby transmitting the footing pressure more effectively to the underlying soil layer. The angle of load dispersion in the geocell mattress is found to increase with decrease in the size of the aperture opening of geogrid.

CONCLUSIONS

Based on the findings from this investigation it could be concluded that the load carrying capacity of the geocell mattress increases with increase in strength of the geogrid used to make geocells. When the geogrid ribs are in horizontal and vertical direction in the geocell wall they effectively resist against footing penetration through mobilisation of vertical compression and horizontal anchorage. With decrease in aperture opening of the geogrid higher confinement and hence higher compressive strength is induced to the encapsulated soil thereby giving rise to better performance improvement.

Acknowledgements: The author would like to thank Professor K. Rajagopal for his valuable comments and suggestions.

Corresponding author: Dr Sujit Kumar Dash, Indian Institute of Technology Guwahati, Department of Civil Engineering, Guwahati - 781 039, India. Tel: 91 361 258 2417. Email: sujit@iitg.ernet.in.

REFERENCES

Bush, D.I., Jenner, C.G. and Bassett, R.H. 1990. The Design and Construction of Geocell Foundation Mattress Supporting Embankments over Soft Ground, Geotextiles and Geomembranes, 9, 83-98.

Cowland. J.W. and Wong, S.C.K. 1993. Performance of a Road Embankment on Soft Clay Supported on a Geocell Mattress Foundation, Geotextiles and Geomembranes, 12, 687-705.

Dash, S.K., Krishnaswamy, N.R., Rajagopal, K. 2001. Bearing Capacity of Strip Footings Supported on Geocell-Reinforced Sand, Geotextiles and Geomembranes, 19, 235-256.

Krishnaswamy, N.R., Rajagopal, K. and Madhavi Latha, G. 2000. Model studies on Geocell Supported Embankments Constructed over Soft Clay Foundation, Geotechnical Testing Journal, ASTM, 23, 45-54.